Macrophage NCOR1 protects from atherosclerosis by repressing a pro-atherogenic PPARγ signature

Oppi, Sara; Nusser-Stein, Stefanie; Blyszczuk, Przemyslaw; Wang, Xu; Jomard, Anne; Marzolla, Vincenzo; Yang, Kangmin; Velagapudi, Srividya; Ward, Liam J; Yuan, Xi-Ming

Published in:
European Heart Journal

DOI:
10.1093/eurheartj/ehz667

ESC European Society of Cardiology

European Heart Journal (2019) **0**, 1–11
doi:10.1093/eurheartj/ehz667

BASIC SCIENCE

Macrophage NCOR1 protects from atherosclerosis by repressing a pro-atherogenic PPARγ signature

Sara Oppi[1], Stefanie Nusser-Stein[1], Przemyslaw Blyszczuk[2,3], Xu Wang[4], Anne Jomard[5,6], Vincenzo Marzolla[1,7], Kangmin Yang[1], Srividya Velagapudi[1], Liam J. Ward[8], Xi-Ming Yuan[8], Martin A. Geiger[9], Ana T. Guillaumon[9], Alaa Othman[6], Thorsten Hornemann[6], Zoran Rancic[10], Dongryeol Ryu[11], Maaike H. Oosterveer[12], Elena Osto[1,5,6], Thomas F. Lüscher[1,13,14], and Sokrates Stein[1]*

[1]Center for Molecular Cardiology, University of Zurich, Wagistrasse 12, 8952 Schlieren, Switzerland; [2]Department of Rheumatology, Center of Experimental Rheumatology, University Hospital Zurich, 8091 Zurich, Switzerland; [3]Department of Clinical Immunology, Jagiellonian University Medical College, 31-008 Cracow, Poland; [4]Department of Plant Science, School of Agriculture and Biology, Shanghai Jiao Tong University, 200240 Shanghai, China; [5]Laboratory of Translational Nutrition Biology, Institute of Food, Nutrition and Health, ETH Zurich, 8603 Schwerzenbach, Switzerland; [6]Institute for Clinical Chemistry, University Hospital Zurich, 8091 Zurich, Switzerland; [7]Laboratory of Cardiovascular Endocrinology, IRCCS San Raffaele Pisana, 00163 Rome, Italy; [8]Department of Clinical and Experimental Medicine, Linköping University, 581 83 Linköping, Sweden; [9]Vascular Diseases Discipline, Clinics Hospital of the University of Campinas, 13083-970 Campinas, Brazil; [10]Clinic for Vascular Surgery, University Hospital Zurich, 8091 Zurich, Switzerland; [11]Department of Molecular Cell Biology, Sungkyunkwan University School of Medicine, 16419 Suwon, Republic of Korea; [12]Department of Pediatrics, Center for Liver Digestive and Metabolic Diseases, University of Groningen, University Medical Center Groningen, 9713 Groningen, The Netherlands; [13]Department of Cardiology, Royal Brompton & Harefield Hospital Trust, London, SW3 6NP, UK; and [14]Imperial College London, London, SW7 2AZ, UK

Received 11 April 2019; revised 28 July 2019; editorial decision 3 September 2019; accepted 4 September 2019

This paper was guest edited by Filippo Crea, Rome

Aims Nuclear receptors and their cofactors regulate key pathophysiological processes in atherosclerosis development. The transcriptional activity of these nuclear receptors is controlled by the nuclear receptor corepressors (NCOR), scaffolding proteins that form the basis of large corepressor complexes. Studies with primary macrophages demonstrated that the deletion of *Ncor1* increases the expression of atherosclerotic molecules. However, the role of nuclear receptor corepressors in atherogenesis is unknown.

Methods and results We generated myeloid cell-specific *Ncor1* knockout mice and crossbred them with *low-density lipoprotein receptor* (*Ldlr*) knockouts to study the role of macrophage NCOR1 in atherosclerosis. We demonstrate that myeloid cell-specific deletion of nuclear receptor corepressor 1 (NCOR1) aggravates atherosclerosis development in mice. Macrophage *Ncor1*-deficiency leads to increased foam cell formation, enhanced expression of pro-inflammatory cytokines, and atherosclerotic lesions characterized by larger necrotic cores and thinner fibrous caps. The immunometabolic effects of NCOR1 are mediated via suppression of peroxisome proliferator-activated receptor gamma (PPARγ) target genes in mouse and human macrophages, which lead to an enhanced expression of the CD36 scavenger receptor and subsequent increase in oxidized low-density lipoprotein uptake in the absence of NCOR1. Interestingly, in human atherosclerotic plaques, the expression of *NCOR1* is reduced whereas the PPARγ signature is increased, and this signature is more pronounced in ruptured compared with non-ruptured carotid plaques.

Conclusions Our findings show that macrophage NCOR1 blocks the pro-atherogenic functions of PPARγ in atherosclerosis and suggest that stabilizing the NCOR1–PPARγ binding could be a promising strategy to block the pro-atherogenic functions of plaque macrophages and lesion progression in atherosclerotic patients.

Keywords

* Corresponding author. Tel: +41 44 635 5094, Fax: +41 44 635 68 27, Email: sokrates.stein@uzh.ch

Atherosclerosis • Immunometabolic disease • Mechanism of disease • Nuclear receptor corepressor • Ncor1

Translational perspective

The development of atherosclerosis is triggered by inflammatory and metabolic cues, whose downstream pathways are connected in immunometabolic networks that are regulated by key transcriptional coregulators, such as nuclear receptor corepressor 1 (NCOR1). This study demonstrates that macrophage NCOR1 represses pro-atherogenic functions of proliferator-activated receptor gamma (PPARγ). Consistently, the deletion of macrophage *Ncor1* aggravates atherosclerosis in mice. Moreover, analyses of human carotid plaque specimens suggest that the NCOR1-driven PPARγ suppression is also protective in human plaque development and vulnerability. Therefore, the defined function of macrophage NCOR1 in atherosclerosis may open new therapeutic strategies to prevent the development and progression of the atherosclerosis and cardiovascular disease.

Introduction

Atherosclerosis develops in the context of dyslipidaemia and chronic inflammation and affects conduit and medium-size muscular arteries of several organs.[1] During disease development, monocytes bind to activated endothelial cells, transmigrate into the sub-intimal space, and differentiate into macrophages.[2] Plaque macrophages interact with other immune cells, accumulate excessive amounts of cholesterol derived from oxidized low-density lipoprotein (oxLDL) particles and become foam cells, thereby promoting plaque formation.[1,2]

Nuclear receptor corepressor 1 (NCOR1) serves as scaffolding protein that forms the basis for a large corepressor complex that acts via suppression of different nuclear receptors, such as liver X receptors (LXRs), peroxisome proliferator-activated receptors (PPARs), and thyroid hormone receptors (THRs).[3] Although germline *Ncor1* knockout mice are embryonically lethal, they served to establish crucial roles for NCOR1 in erythropoiesis, T-cell, and central nervous system development.[4] Recent studies using truncated versions or tissue-specific deletions of NCOR1 demonstrated that this transcriptional corepressor impacts on muscle mass and mitochondrial function, improves insulin sensitivity in adipose tissue, and regulates intestinal cholesterol absorption.[5–9]

Methods

Animal studies and ethics

We crossbred floxed *Ncor1* mice ($Ncor1^{fl/fl}$)[8] with mice expressing Cre recombinase driven by the lysozyme M promoter ($Lyz2^{tm1(cre)Ifo}$)[10] to obtain myeloid cell-specific *Ncor1* knockouts ($Ncor1^{Mye-/-}$ knockouts and $Ncor1^{Mye+/+}$ control mice). These mice were then further crossbred to *low-density lipoprotein* receptor knockout mice ($Ldlr^{tm1Her}$)[11] to bring them into an atherosclerosis-prone background, i.e. $L\text{-}Ncor1^{Mye-/-}$ knockouts and $L\text{-}Ncor1^{Mye+/+}$ control mice. All animal procedures were approved by the Swiss authorities (Canton of Zurich, animal protocol ZH061/16) and performed in accordance with our institutional guidelines.

Human ethics

Patients with asymptomatic or symptomatic carotid occlusive disease were referred to the Clinic for Cardiovascular Surgery of the University Hospital of Zurich (Zurich, Switzerland) for carotid endarterectomy as previously described.[12] Written informed consent was obtained from all patients, plaque specimens were anonymized, and the baseline characteristics of the patients were described by Müller *et al.*[12] Plaques were classified as non-ruptured or ruptured according to published guidelines.[13,14]

Statistics

Statistical analysis was performed with GraphPad Prism (version 6). Data are expressed as scatter plots of individual values with the mean or box plots with the full range of variation (from min. to max.), the inter-quartile range and the median. Analysis of *en face* atherosclerotic plaque content was carried out with unpaired, non-parametric Mann–Whitney *U t*-tests. Comparison of differences between two groups of other experiments was assessed using unpaired two-tailed (multiple) Student's *t*-tests. Multiple group comparisons were assessed by two-way analysis of variance (ANOVA) and Bonferroni's *post hoc t*-tests. Adjusted *P*-values were calculated by multiplying raw *P*-values by *g*, where *g* indicates the number of comparisons.

The complete ethics sections and methods are specified in the Supplementary material online.

Results

Myeloid cell-specific deletion of Ncor1 aggravates atherosclerosis development

Since previous studies demonstrated that macrophage NCOR1 is required for the PPARγ or LXR-mediated transrepression of pro-inflammatory molecules,[15–17] we speculated that NCOR1 exerts a protective function during atherosclerosis development. To first verify if NCOR1 plays a role in human atherosclerosis, we compared transcriptomic data from human carotid plaques obtained from patients undergoing carotid endarterectomy.[18] NCOR1, as well as its strong binding partner histone deacetylase 3 (HDAC3), showed several strong correlations with various transcripts that are known to affect atherosclerosis development (*Figure 1A* and Supplementary material online, *Figure S1*), suggesting that it might regulate plaque development. For example, the *NCOR1* expression correlates with

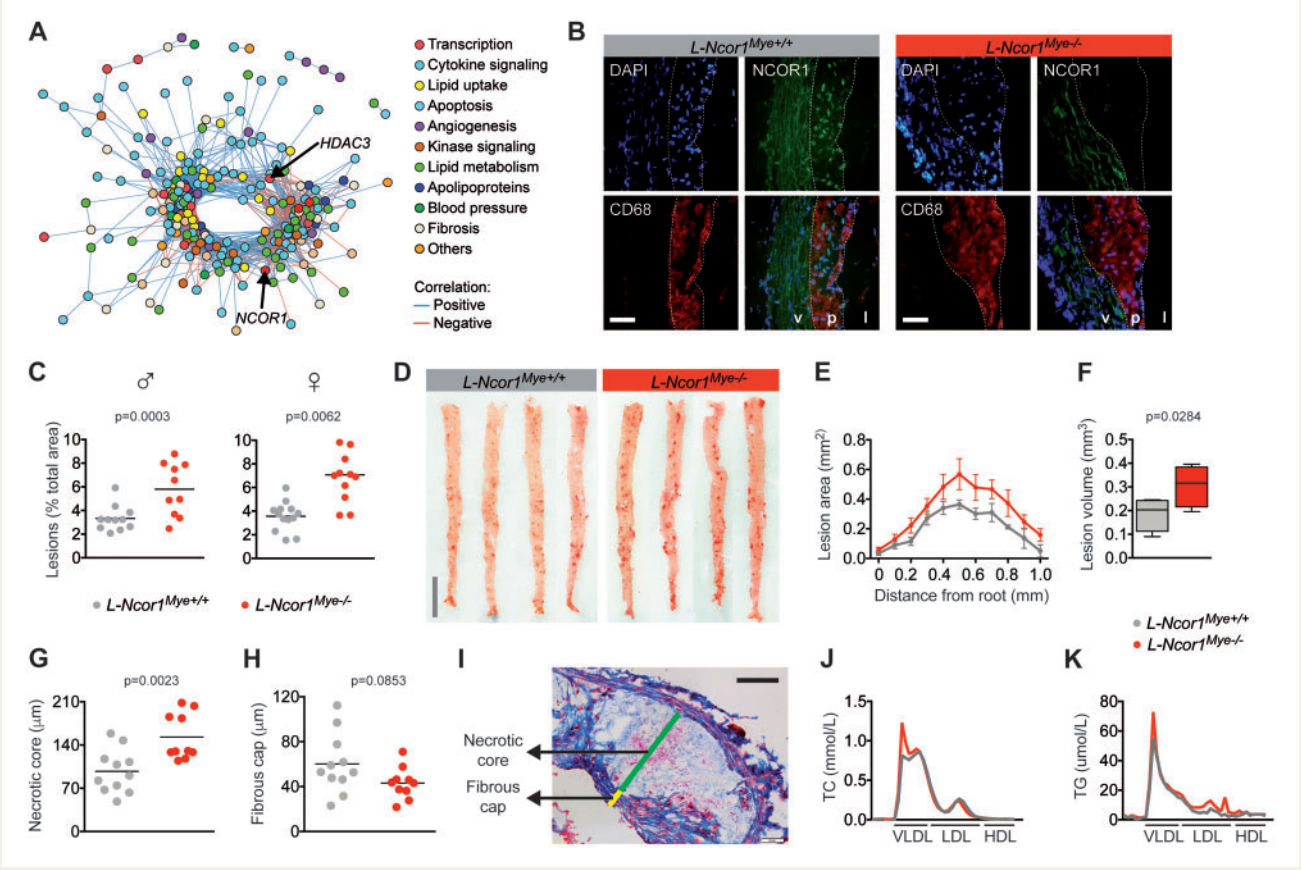

Figure 1 Myeloid cell-specific deletion of *Ncor1* promotes atherosclerosis development and the formation of lesions with advanced signs of plaque vulnerability. (*A*) Correlation network of transcripts that affect atherosclerosis development in human carotid plaques. Spearman's correlation, Rho >0.6, $P < 1e\text{-}10$ (raw data, GSE21545). (*B*) Representative staining for NCOR1 (green), CD68 (red), and DAPI (blue) in cross-sections of aortic sinus plaques from *L-Ncor1*$^{Mye+/+}$ and *L-Ncor1*$^{Mye-/-}$ mice. l, lumen; p, plaque; v, vascular smooth muscle cells. Scale bar, 200 µm. (*C*) Quantification of atherosclerotic plaques in thoraco-abdominal aortae of male and female *L-Ncor1*$^{Mye+/+}$ and *L-Ncor1*$^{Mye-/-}$ mice. $n = 11$ male *L-Ncor1*$^{Mye+/+}$; $n = 10$ male *L-Ncor1*$^{Mye-/-}$; $n = 13$ female *L-Ncor1*$^{Mye+/+}$; $n = 11$ female *L-Ncor1*$^{Mye-/-}$. (*D*) Representative images of Oil-red O stained thoraco-abdominal aortae of male *L-Ncor1*$^{Mye+/+}$ and *L-Ncor1*$^{Mye-/-}$ mice. Scale bar, 5 mm. (*E, F*) Quantification of atherosclerotic lesion area through the aortic sinus and ascending aorta from *L-Ncor1*$^{Mye+/+}$ and *L-Ncor1*$^{Mye-/-}$ mice: (*E*) mean lesion area ± SEM, and (*F*) volume of the aortic sinus lesions represented in box plots (min. to max. values and median). $n = 6$ *L-Ncor1*$^{Mye+/+}$; $n = 5$ *L-Ncor1*$^{Mye-/-}$ mice. (*G, H*) Quantification of the necrotic core size (*G*) and the protective fibrous cap (*H*) in cross-sections of aortic sinus plaques from *L-Ncor1*$^{Mye+/+}$ ($n = 11$) and *L-Ncor1*$^{Mye-/-}$ ($n = 10$) mice. (*I*) Representative images displaying the necrotic core and fibrous cap. Scale bar, 100 µm. (*J, K*) Cholesterol (*J*) and triglyceride (*K*) content in lipoprotein subfractions. HDL, high-density lipoprotein; LDL, low-density lipoprotein; VLDL, very low-density lipoprotein. $n = 1$ pooled sample from six mice per genotype. Data are represented in scatter plots with means. Displayed *P*-value relative to *L-Ncor1*$^{Mye+/+}$, as determined by Student's *t*-test.

transcripts regulating lipid metabolism, such as *FDT1*, *INSIG2*, and *IDI1*, and apoptotic regulators, such as *BAG3*, *PTPN13*, and *FAS* (Supplementary material online, *Figure S1*).

In order to evaluate the contribution of macrophage NCOR1 in atherosclerosis, we generated myeloid cell-specific *Ncor1* knockout mice[8,9] on an atherosclerosis-prone *Ldlr*$^{-/-}$ background (described here as *L-Ncor1*$^{Mye-/-}$ and control mice as *L-Ncor1*$^{Mye+/+}$), and exposed them to a high-cholesterol diet for 12 weeks. The efficient myeloid deletion of NCOR1 was clearly detectable in plaque macrophages and isolated peritoneal macrophages from *L-Ncor1*$^{Mye-/-}$ mice at RNA and protein level (*Figure 1B* and Supplementary material online, *Figure S2* and *S3*). Prior to exposure to high-cholesterol diet, cholesterol and triglycerides plasma levels were not altered between male (Supplementary material online, *Figure S4A*), but slightly higher in female *L-Ncor1*$^{Mye-/-}$ compared with *L-Ncor1*$^{Mye+/+}$ mice (Supplementary material online, *Figure S4B*). Pre-diet haematological analysis revealed no change in the total number of major blood cell populations, but a higher percentage of neutrophils and a reduced number of lymphocytes among leucocytes in *L-Ncor1*$^{Mye-/-}$ compared with *L-Ncor1*$^{Mye+/+}$ mice (Supplementary material online, *Table S1*). Since neutrophils can affect the development of the disease,[19] we measured neutrophil NETosis to assess their activation and function. No difference was observed in NETosis between *L-Ncor1*$^{Mye-/-}$ and *L-Ncor1*$^{Mye+/+}$ neutrophils (Supplementary material online, *Figure S5*). The body weight was comparable before, during, and after the diet in both genders (Supplementary material online, *Figure S6A–C*).

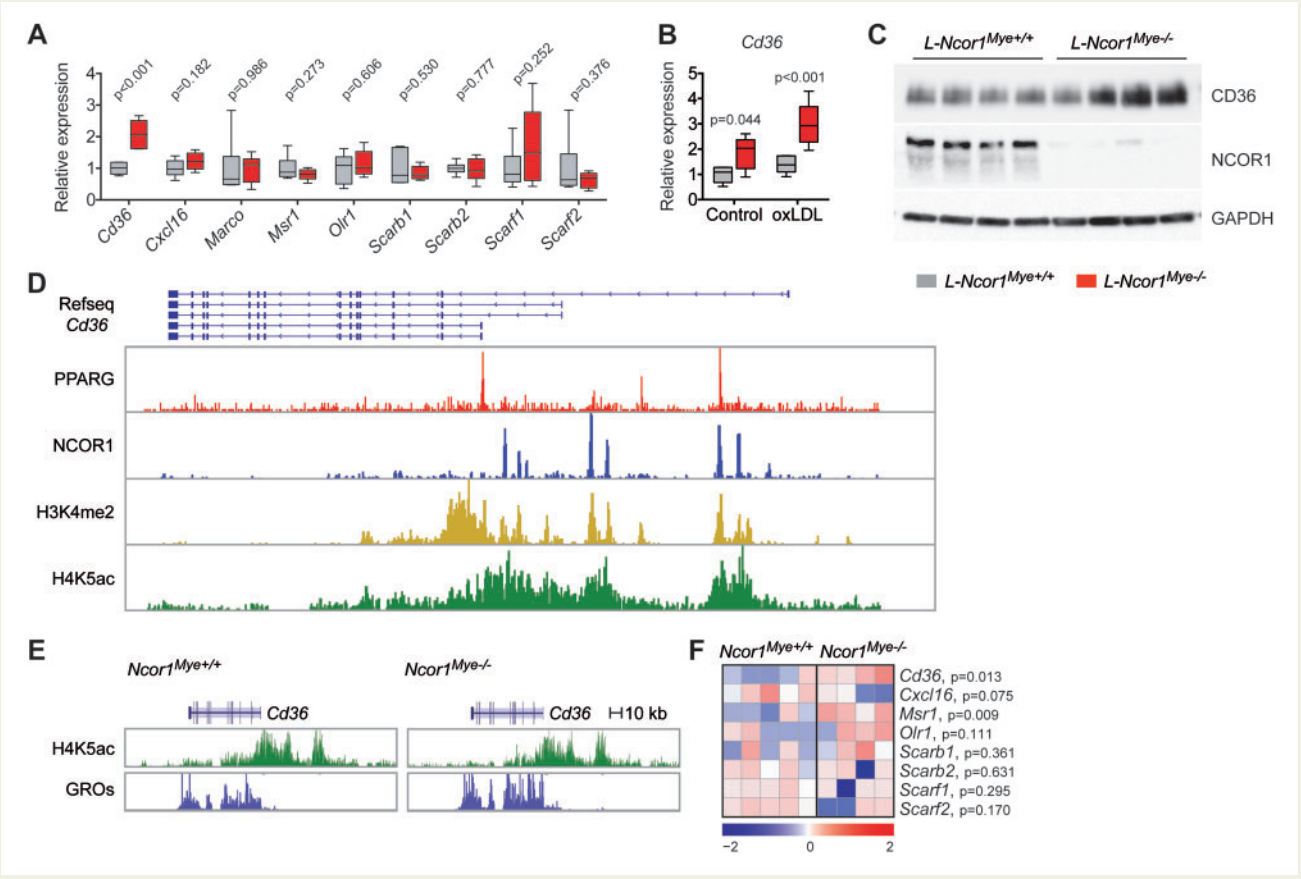

Figure 2 Macrophage NCOR1 promotes the expression of the scavenger receptor CD36. (*A*) The expression of genes regulating cholesterol and lipoprotein transport in the aortic arch of *L-Ncor1*$^{Mye+/+}$ and *L-Ncor1*$^{Mye-/-}$ mice. $n = 6$ mice per genotype. (*B*) The expression of *Cd36* in untreated or overnight oxLDL-treated thioglycolate-elicited peritoneal macrophages. $n = 6$ *L-Ncor1*$^{Mye+/+}$; $n = 9$ *L-Ncor1*$^{Mye-/-}$. (*C*). Immunoblots of CD36, NCOR1, and GAPDH on macrophage lysates from *L-Ncor1*$^{Mye+/+}$ and *L-Ncor1*$^{Mye-/-}$ mice. (*D*) ChIP-seq data displaying binding sites of NCOR1, PPARγ, H3K4m2, and H4K5ac in peritoneal macrophages of wild-type mice (raw data, GSE21314, GSE27033, GSE50944). (*E*) ChIP-seq data displaying H4K5ac binding and GRO sequencing in *Ncor1*$^{Mye+/+}$ and *Ncor1*$^{Mye-/-}$ macrophages (raw data, GSE27033, GSE50944). (*F*) Heatmap displaying normalized GRO-seq counts in the transcribed genetic area of the indicated scavenger receptors. Log_2 scale as *z*-scores (raw data, GSE50944). Data are represented in box plots (min. to max. values and median). (Adjusted, $P \times g$) *P*-values relative to *L-Ncor1*$^{Mye+/+}$ (or described in image), as determined by (multiple) Student's *t*-tests or two-way ANOVA and Bonferroni's *post hoc t*-tests.

Importantly, both male and female *L-Ncor1*$^{Mye-/-}$ mice developed more atherosclerotic lesions in thoraco-abdominal aortae than control *L-Ncor1*$^{Mye+/+}$ mice (*Figure 1C, D*). Moreover, lesions at the aortic sinus of *L-Ncor1*$^{Mye-/-}$ mice were larger, contained more lipids, and displayed increased CD68 staining (*Figure 1E, F* and Supplementary material online, *Figure S7A–E*). In addition, atherosclerotic lesions of *L-Ncor1*$^{Mye-/-}$ mice displayed advanced signs of plaque vulnerability compared with *L-Ncor1*$^{Mye+/+}$ mice, characterized by larger necrotic cores and thinner fibrous caps (*Figure 1G–I*). Lipoprotein fractioning after the diet revealed slightly increased cholesterol levels in very low-density lipoprotein fractions of *L-Ncor1*$^{Mye-/-}$ mice, while triglycerides were not changed (*Figure 1J, K*). Furthermore, the numbers of major blood cell populations were comparable in both genotypes (Supplementary material online, *Figure S8A–H*), but *L-Ncor1*$^{Mye-/-}$ mice had increased plasma levels of various inflammatory cytokines compared with *L-Ncor1*$^{Mye+/+}$ mice (Supplementary material online, *Figure S9*).

Increased expression of CD36 in aortae of myeloid cell-specific Ncor1 knockouts

We next analysed the expression of atherosclerosis-associated transcripts, including genes involved in cholesterol transport, inflammation, and lipogenesis, in the aortic arch of *L-Ncor1*$^{Mye-/-}$ compared with *L-Ncor1*$^{Mye+/+}$ mice. Surprisingly, only the expression of *Cd36* was robustly increased in *L-Ncor1*$^{Mye-/-}$ compared with *L-Ncor1*$^{Mye+/+}$ mice, while the expression of most other genes of interest was not altered (*Figure 2A* and Supplementary material online, *Figure S10*). CD36 (also known as fatty acid translocase) is an important scavenger receptor that mediates the uptake of oxLDL particles into

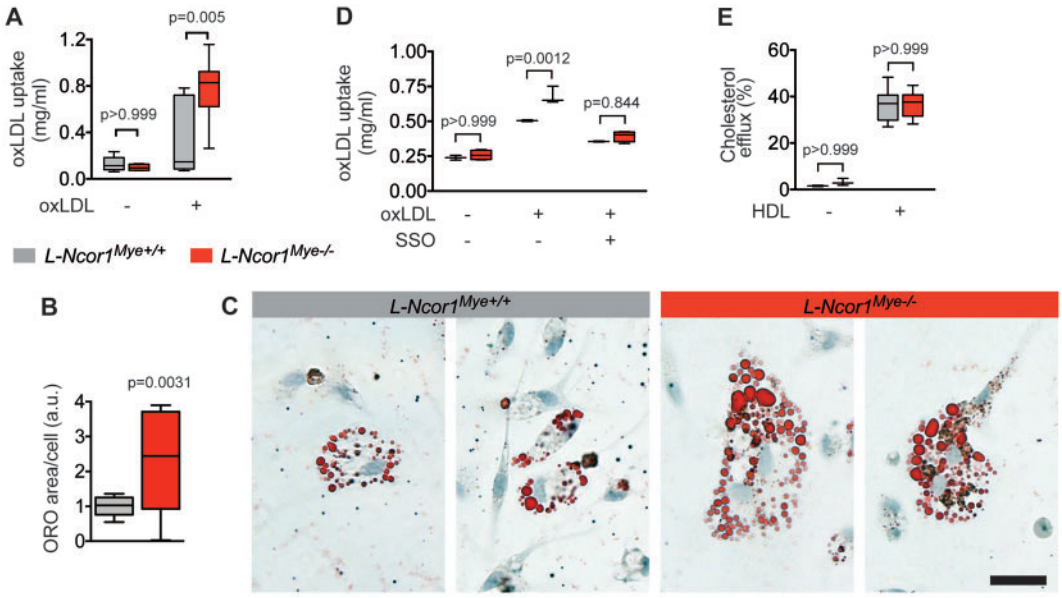

Figure 3 Myeloid cell-specific deletion of *Ncor1* promotes CD36-mediated uptake of oxLDL. (*A*) Quantification of oxLDL uptake in peritoneal macrophages of *L-Ncor1*$^{Mye+/+}$ and *L-Ncor1*$^{Mye-/-}$ mice upon 4 h DiI-oxLDL stimulation. $n \geq 4$ per genotype. (*B*) Evaluation of lipid droplet content in *L-Ncor1*$^{Mye+/+}$ and *L-Ncor1*$^{Mye-/-}$ peritoneal macrophages as determined by Oil-red O staining and quantification upon 8 h DiI-oxLDL stimulation. $n \geq 10$ microscopic fields per genotype. (*C*) Representative images displaying the lipid droplets. Scale bar, 20 µm. (*D*) Assessment of oxLDL uptake in peritoneal macrophages that were treated with SSO for 30 min prior to stimulation with DiI-oxLDL for 4 h. $n = 2$ untreated, $n = 4$ SSO-treated per genotype. (*E*) Analysis of HDL-driven cholesterol efflux from *L-Ncor1*$^{Mye+/+}$ and *L-Ncor1*$^{Mye-/-}$ peritoneal macrophages. $n = 3$ untreated, $n = 8$ HDL-stimulated per genotype. Data are represented in box plots (min. to max. values and median). (Adjusted, $P \times g$) *P*-values relative to *L-Ncor1*$^{Mye+/+}$, as determined by (multiple) Student's *t*-tests or two-way ANOVA and Bonferroni's *post hoc t*-tests.

macrophages and thereby promotes atherosclerosis development.[20–22] The increase of CD36 expression could be secondary to an enhanced accumulation of CD36^{+} macrophages and/or a higher expression of *Cd36* in individual plaque macrophages. Flow cytometry analyses of atherosclerotic aortae revealed that the content of CD45^{+} immune cells is comparable in the two genotypes (Supplementary material online, *Figure S11A, B*), and that about 50% of these cells are CD36^{+} macrophages (Supplementary material online, *Figure S11C, D*), suggesting that the accumulation of monocyte-derived macrophages in aortic lesions is comparable in the two genotypes. Moreover, no major differences were observed in the content of other myeloid cell populations, including monocytes, neutrophils, and eosinophils (Supplementary material online, *Figure S11C*).

Macrophage NCOR1 directly regulates the PPARγ-driven expression of CD36

To verify if the increased expression of *Cd36* is indeed cell-autonomous, we analysed its expression in aortae of young mice under a normal chow diet (which do not have any atherosclerotic lesions) and in thioglycolate-elicited peritoneal macrophages. The expression of *Cd36* and inflammatory endothelial cell markers was not altered in aortae of young mice (Supplementary material online, *Figure S12*). In contrast, *Cd36* expression was enhanced in *L-Ncor1*$^{Mye-/-}$ compared with *L-Ncor1*$^{Mye+/+}$ peritoneal macrophages under basal conditions (*Figure 2B, C*), and further increased upon stimulation with oxLDL (*Figure 2B*). These data indicate that *Cd36* is specifically up-regulated in macrophages and not in other vascular cells.

We next analysed NCOR1, H3K4me2, H4K5ac, and global run-on (GRO) ChIP-seq data from *Ncor1*$^{Mye-/-}$ and *Ncor1*$^{Mye+/+}$ peritoneal macrophages from available datasets.[5,23,24] Our analysis identified NCOR1 recruitment to different sites of the *Cd36* promoter region (*Figure 2D*). These sites also displayed enhanced signals for H3K4 dimethylation and H4K5 acetylation, as well as PPARγ binding to one NCOR1-enriched sites (*Figure 2D*), suggesting that the promoter is in an active status. Interestingly, increased *de novo* transcription rates were observed at the *Cd36* gene of *Ncor1*$^{Mye-/-}$ compared with *Ncor1*$^{Mye+/+}$ peritoneal macrophages (*Figure 2E, F*), showing that macrophage NCOR1 directly affects the expression of *Cd36*.

CD36 promotes oxLDL accumulation in Ncor1-deficient macrophages

To assess a functional contribution of CD36 to the phenotype of the *L-Ncor1*$^{Mye-/-}$ mice, we isolated peritoneal macrophages and exposed them to oxLDL *ex vivo*. Notably, macrophages from *L-Ncor1*$^{Mye-/-}$ mice accumulated more oxLDL than *L-Ncor1*$^{Mye+/+}$ macrophages (*Figure 3A*). To measure lipid droplet formation, we stimulated peritoneal macrophages with oxLDL and performed Oil-red O staining. Consistent with the increased uptake of oxLDL, we do observe increased lipid droplet formation in L-Ncor1$^{Mye-/-}$ compared with L-Ncor1$^{Mye+/+}$ peritoneal macrophages (*Figure 3B, C*). The accumulation of cholesterol in macrophages is dependent on the uptake,

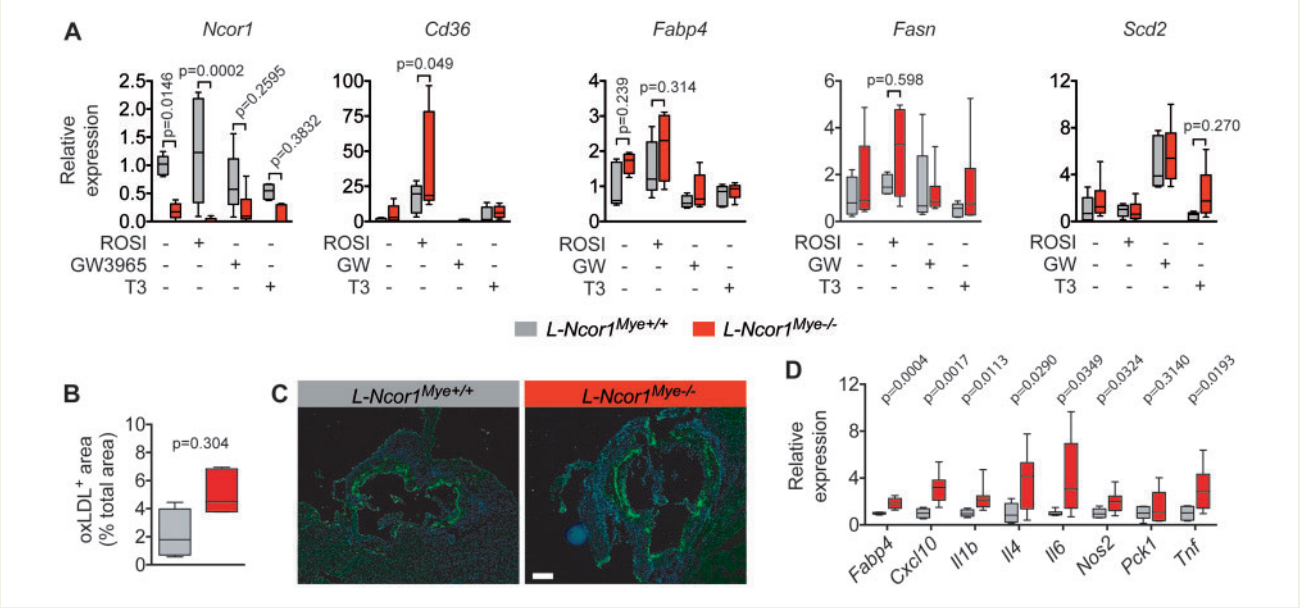

Figure 4 The deleterious effects of macrophage *Ncor1* deficiency are mediated via de-repression of PPARγ. (*A*) Relative expression of *Ncor1*, *Cd36*, *Fabp4*, *Fasn*, and *Scd2* in peritoneal macrophages of *L-Ncor1*$^{Mye+/+}$ and *L-Ncor1*$^{Mye-/-}$ mice undergoing stimulation with different nuclear receptor agonists for 16 h. $n \geq 4$ per genotype. ROSI, rosiglitazone; GW, GW3965; T3, triiodothyronine. (*B*) oxLDL-positive in aortic sinus lesions from *L-Ncor1*$^{Mye+/+}$ and *L-Ncor1*$^{Mye-/-}$ mice. $n \geq 4$ per genotype. (*C*) Representative images of the oxLDL immunostainings in aortic sinus lesions from *L-Ncor1*$^{Mye+/+}$ and *L-Ncor1*$^{Mye-/-}$ mice. Scale bar, 200 µm. (*D*) The expression of various inflammatory and PPARγ target genes in peritoneal macrophages stimulated with rosiglitazone for 16 h. $n = 6$ *L-Ncor1*$^{Mye+/+}$; $n = 9$ *L-Ncor1*$^{Mye-/-}$. Data are represented in box plots (min. to max. values and median). (Adjusted, $P \times g$) *P*-values relative to *L-Ncor1*$^{Mye+/+}$, as determined by (multiple) Student's *t*-tests or two-way ANOVA and Bonferroni's *post hoc t*-tests. For all *P*-values that are not displayed the value is $P > 0.999$.

esterification, and storage in lipid droplets, as well as by their hydrolysis and efflux. Interestingly, the increased uptake of oxLDL could be blocked by treating macrophages with the CD36 inhibitor sulfo-N-succinimidyl oleate (SSO)[25] (*Figure 3D*). Moreover, we did not observe any difference in macrophage cholesterol efflux (*Figure 3E*), suggesting that the increased foam cell formation is a consequence of a specifically increased CD36-mediated oxLDL uptake.

PPARγ is a nuclear receptor that regulates the expression of *Cd36*, foam cell formation, and interacts with NCOR1[17,26–28]. As noted before, we observed an overlapping ChIP-seq peak for PPARγ and NCOR1 at the *Cd36* promoter region (*Figure 2D*). Two further nuclear receptors that interact with NCOR1 and play important roles in macrophages are LXRs and TRβ.[5–7] We, therefore, used agonists to activate PPARγ, LXR, or TRβ, and assessed the downstream effects on *Cd36* expression and other targets in peritoneal macrophages. The expression of *Cd36* was clearly induced upon PPARγ activation and further augmented in *L-Ncor1*$^{Mye-/-}$ compared with *L-Ncor1*$^{Mye+/+}$ macrophages, while LXR and TRβ activators had no effects (*Figure 4A*). Another PPARγ target gene, *fatty acid binding protein 4* (*Fabp4*, also known as *aP2*), displayed a trend to be increased in *L-Ncor1*$^{Mye-/-}$ macrophages as well, suggesting that NCOR1 deficiency leads to a de-repression of PPARγ target genes (*Figure 4A*). On the other hand, the LXR target genes *fatty acid synthase* (*Fasn*) and *stearoyl-Coenzyme A desaturase 2* (*Scd2*) were not changed upon LXR activation between the two genotypes (*Figure 4A*), proposing that the deletion of NCOR1 in macrophage primarily affects the function of PPARγ.

De-repression of PPARγ target genes in the absence of NCOR1

Noteworthy, PPARγ does not only induce the expression of CD36 but also the function of PPARγ itself is stimulated by oxidized metabolites of linoleic acid derived from oxLDL particles,[27] which are chronic pro-atherogenic triggers. Interestingly, the content of oxLDL particles in aortic sinus lesions was higher in *L-Ncor1*$^{Mye-/-}$ compared with *L-Ncor1*$^{Mye+/+}$ mice (*Figure 4B, C*). We, therefore, wondered if the stimulation of PPARγ would resemble a pro-atherogenic inflammatory response in *L-Ncor1*$^{Mye-/-}$ macrophages. Indeed, the expression of direct PPARγ target genes and pro-inflammatory mediators was increased upon PPARγ stimulation in *L-Ncor1*$^{Mye-/-}$ compared with *L-Ncor1*$^{Mye+/+}$ macrophages (*Figure 4D*). These findings confirm that NCOR1 is not only required for the PPARγ-mediated repression of nuclear factor kappa B (NF- κB) and activated protein-1 (AP-1) and their pro-inflammatory target genes[17] but it also represses direct PPARγ target genes. Consequently, the deletion of NCOR1 in macrophages leads to a low-grade inflammatory phenotype upon PPARγ stimulation, which resembles the environment within an atherosclerotic plaque.

Besides inducing the expression of CD36 and promoting foam cell formation, PPARγ does also exert anti-atherosclerotic functions, such as alternative macrophage-polarization.[29] Consistently, stimulation of peritoneal macrophages with rosiglitazone increased the mRNA expression of alternative macrophage-polarization markers as well as Arginase-1 activity in *L-Ncor1*$^{Mye-/-}$ compared with

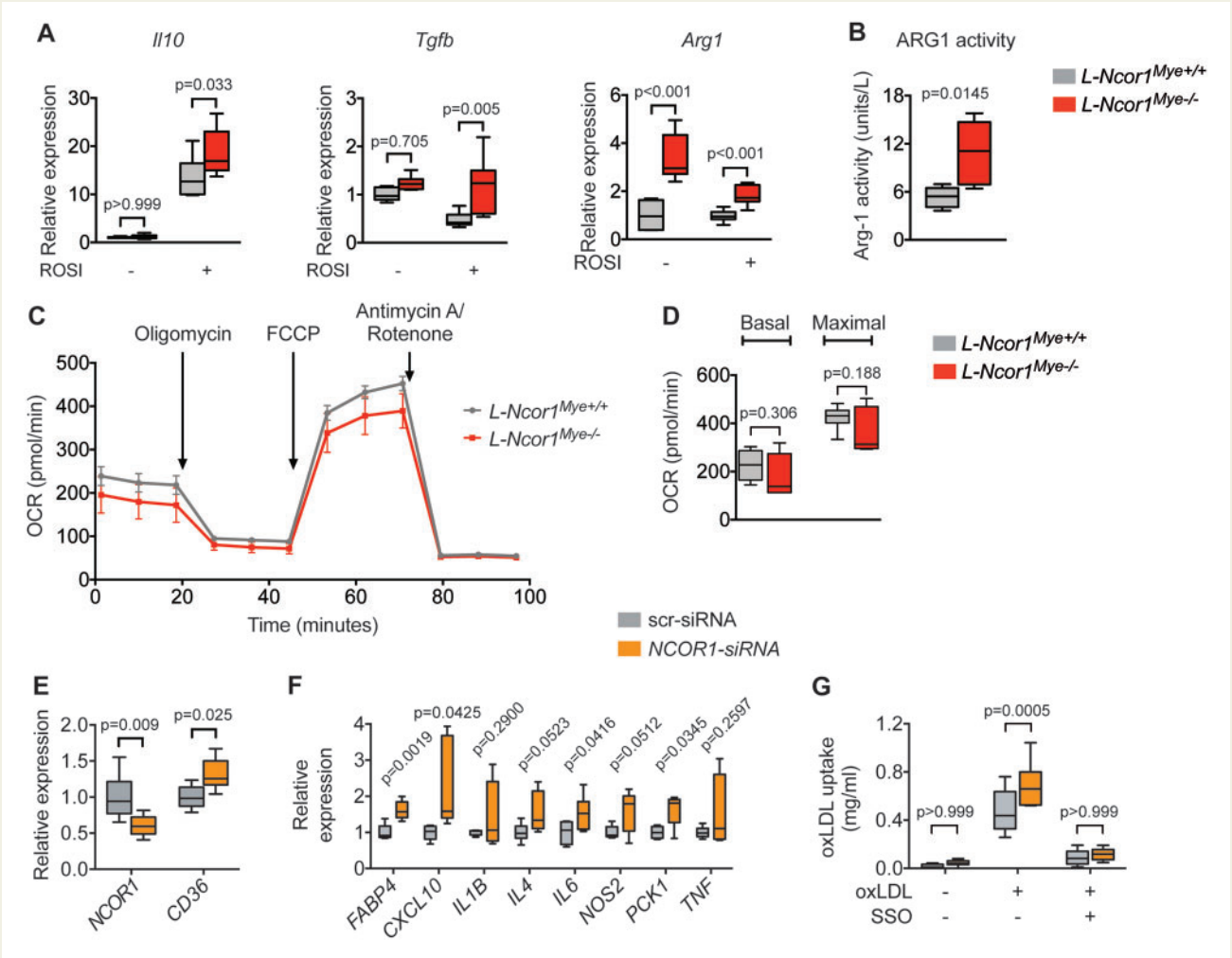

Figure 5 Effects of myeloid cell-specific deletion of *Ncor1* on macrophage polarization and mitochondrial respiration. (*A*) mRNA expression of alternative macrophage-polarization markers in *L-Ncor1*$^{Mye+/+}$ and *L-Ncor1*$^{Mye-/-}$ peritoneal macrophages with or without rosiglitazone (ROSI) treatment. (*B*) Arginase-1 activity in *L-Ncor1*$^{Mye+/+}$ and *L-Ncor1*$^{Mye-/-}$ peritoneal macrophages. (*C*) Oxygen consumption rate (OCR) in peritoneal macrophages that were seeded in Seahorse XF-24 cell culture microplates. Upon overnight incubation, the cells were sequentially treated with oligomycin, FCCP, and antimycin A plus rotenone. (*D*) Quantification of basal and maximal OCR. (*E*) Analysis of *NCOR1* and *CD36* expression in PMA-differentiated THP-1 macrophages that were treated with scrambled or *NCOR1*-siRNA. $n = 6$ per genotype. (*F*) The expression of various inflammatory and direct PPARγ target genes in PMA-differentiated THP-1 macrophages. $n = 6$ per genotype. (*G*) Uptake of oxLDL in PMA-differentiated THP-1 macrophages that were treated with scrambled or *NCOR1*-siRNA, and SSO 30 min before stimulation with DiI-oxLDL for 4 h. $n = 9$ per genotype. Data are represented in box plots (min. to max. values and median). (Adjusted, $P \times g$) *P*-values relative to *L-Ncor1*$^{Mye+/+}$, as determined by (multiple) Student's *t*-tests or two-way ANOVA and Bonferroni *post hoc t*-tests.

L-Ncor1$^{Mye+/+}$ macrophages (*Figure 5A, B*). Nevertheless, the pro-atherosclerotic effects of the CD36-mediated oxLDL uptake seem to overweight these potentially beneficial effects.

To evaluate if the increased expression of CD36 in *L-Ncor1*$^{Mye-/-}$ mice leads to an overload of lipids that could affect the mitochondrial function, we measured the oxygen consumption rate using a mitochondrial stress test in *L-Ncor1*$^{Mye+/+}$ and *L-Ncor1*$^{Mye-/-}$ peritoneal macrophages. Mitochondrial stress studies revealed no significant differences in oxygen consumption rate as well as basal or maximal respiration (*Figure 5C, D*), which is consistent with a previous study using *Cd36*-deficient mice.[30] Moreover, we did not observe any difference in mitochondrial superoxide production between *Ncor1*$^{Mye+/+}$ and *L-Ncor1*$^{Mye-/-}$ peritoneal macrophages (Supplementary material online, *Figure S13*).

CD36-mediated oxLDL uptake in human macrophages upon NCOR1 silencing

To evaluate if the NCOR1-CD36 axis could play a role in human atherosclerosis, we first analysed the impact of *NCOR1* silencing in macrophages derived from the human monocytoid THP-1 cell line. Consistent with the mouse data, silencing of *NCOR1* in PMA-differentiated THP-1 cells increased the expression of *CD36*, other PPARγ-target genes and inflammatory cytokines (*Figure 5E, F*), and

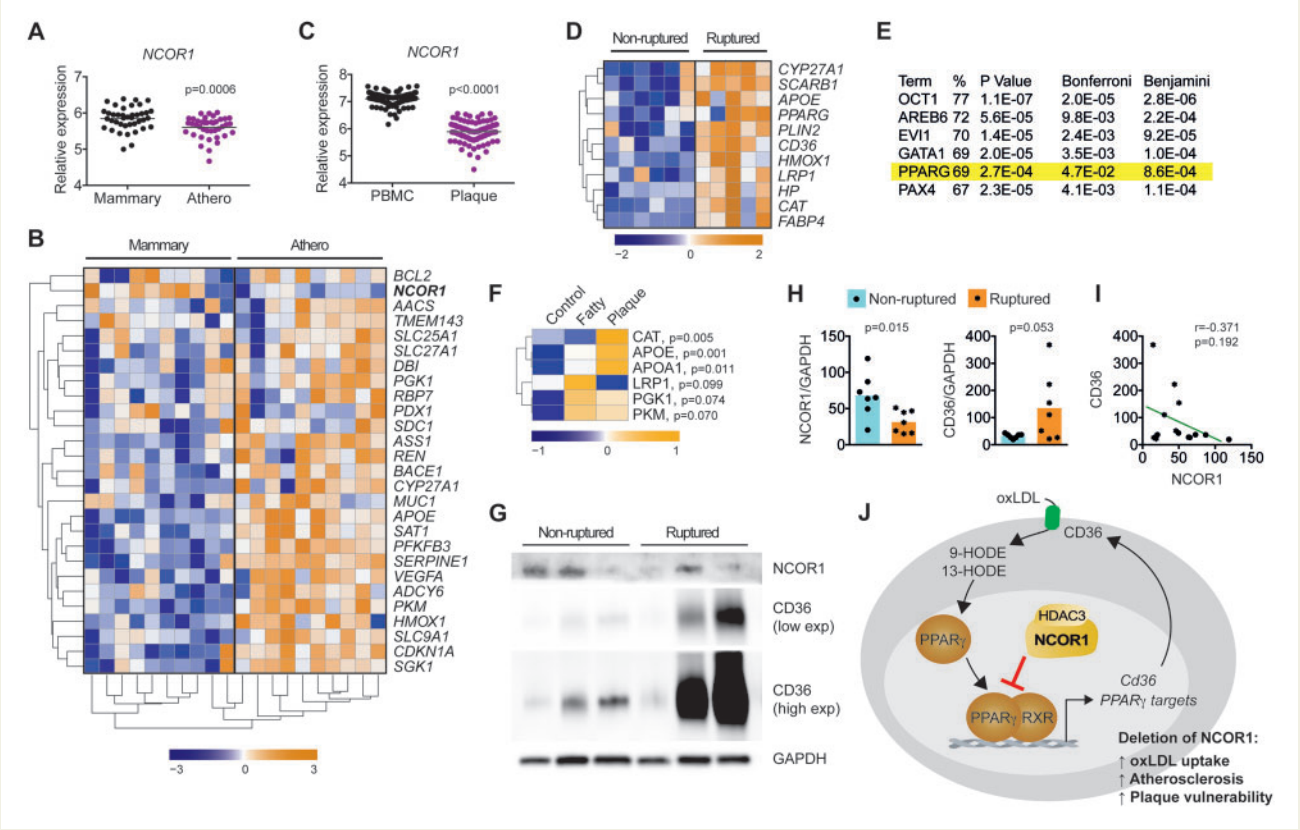

Figure 6 The NCOR1–PPARγ axis in human atherosclerotic disease. (*A, B*) The expression of *NCOR1* (*A*) and PPARγ target genes (*B*) in biopsies of non-atherosclerotic mammary arteries (mammary) and atherosclerotic aortic roots (athero; raw data, GSE40231). $n = 20$ mammary, $n = 20$ athero, $\log_2$ scale as *z*-scores. (*C*) The expression of *NCOR1* in PBMCs or carotid plaques (raw data, GSE21545). $\log_2$ scale. (*D*) Heatmap displaying the relative expression of *NCOR1* and PPARγ target genes in non-ruptured and ruptured human carotid plaques (raw data, GSE41571). $P < 0.05$ non-ruptured relative to ruptured plaque for all transcripts. $n = 6$ non-ruptured, $n = 5$ ruptured plaques, $\log_2$ scale as *z*-scores. (*E*) Analysis of transcription factor-binding sites (TFBS) for the top 1000 *NCOR1*-correlates from GSE41571. (*F*) Heatmap depicting protein expression of identified PPARγ target genes between lesion sites per protein from nLC-MS/MS data analysis. Carotid endarterectomy lesions ($n = 20$, equal gender ratio) were sampled and defined regions isolated: internal control, fatty streak, and plaque centre. $^*P < 0.05$ plaque relative to control. (*G*) Western blot of NCOR1, CD36, and GAPDH on non-ruptured and ruptured atherosclerotic plaques obtained from patients undergoing carotid endarterectomy. A second blot with more samples is shown in Supplementary material online, *Figure S17*. (*H*) Quantification of NCOR1 and CD36 in non-ruptured and ruptured atherosclerotic plaques. $n = 7$ per group. (*I*) Correlation between NCOR1 and CD36 in carotid plaques. Pearson correlation coefficient is displayed. (*J*) Model describing the impact of macrophage *Ncor1* deletion in atherosclerotic disease. Data are represented in scatter plots with means. Displayed *P*-value relative to control group, as determined by Student's *t*-test.

this effect could be partially reverted by inhibiting PPARγ with a specific antagonist (Supplementary material online, *Figure S14*). Consequently, PMA-differentiated THP-1 cells took up more oxLDL, and this effect was blocked by inhibiting the function of CD36 using SSO (*Figure 5G*). Taken together, these data demonstrate that NCOR1 also blocks the PPARγ-mediated expression of *CD36* and the subsequent CD36-mediated uptake of oxLDL in human macrophages.

Reduced expression of NCOR1 and enhanced PPARγ signature in human plaques

We used Coexpedia (www.coexpedia.org) as a resource to explore publicly available array-based transcriptomics data in context with biomedical processes.[31] Gene set analysis identified the 'cellular lipid metabolic process' (GO:0044255, $P = 3.56e\text{-}6$) as the second most relevant biological process for human NCOR1. We next analysed the expression of *NCOR1* and PPARγ target genes in different human cohort studies. Comparison of the gene signature in non-atherosclerotic mammary arteries vs. atherosclerotic aortic roots from the Stockholm Atherosclerosis Gene Expression (STAGE)[32] study revealed a lower expression of *NCOR1* and an increased expression of most PPARγ target genes in atherosclerotic vs. normal vessels (*Figure 6A, B*). A similar observation was done when we analysed the data from peripheral blood mononuclear cells (PBMCs) and carotid plaques from the Biobank of Karolinska Endarterectomy (BiKE) study[18] (*Figure 6C* and Supplementary material online, *Figure S15*), suggesting that a diminished expression of *NCOR1* and an increased PPARγ signature is a general characteristic of atherosclerotic vessels.

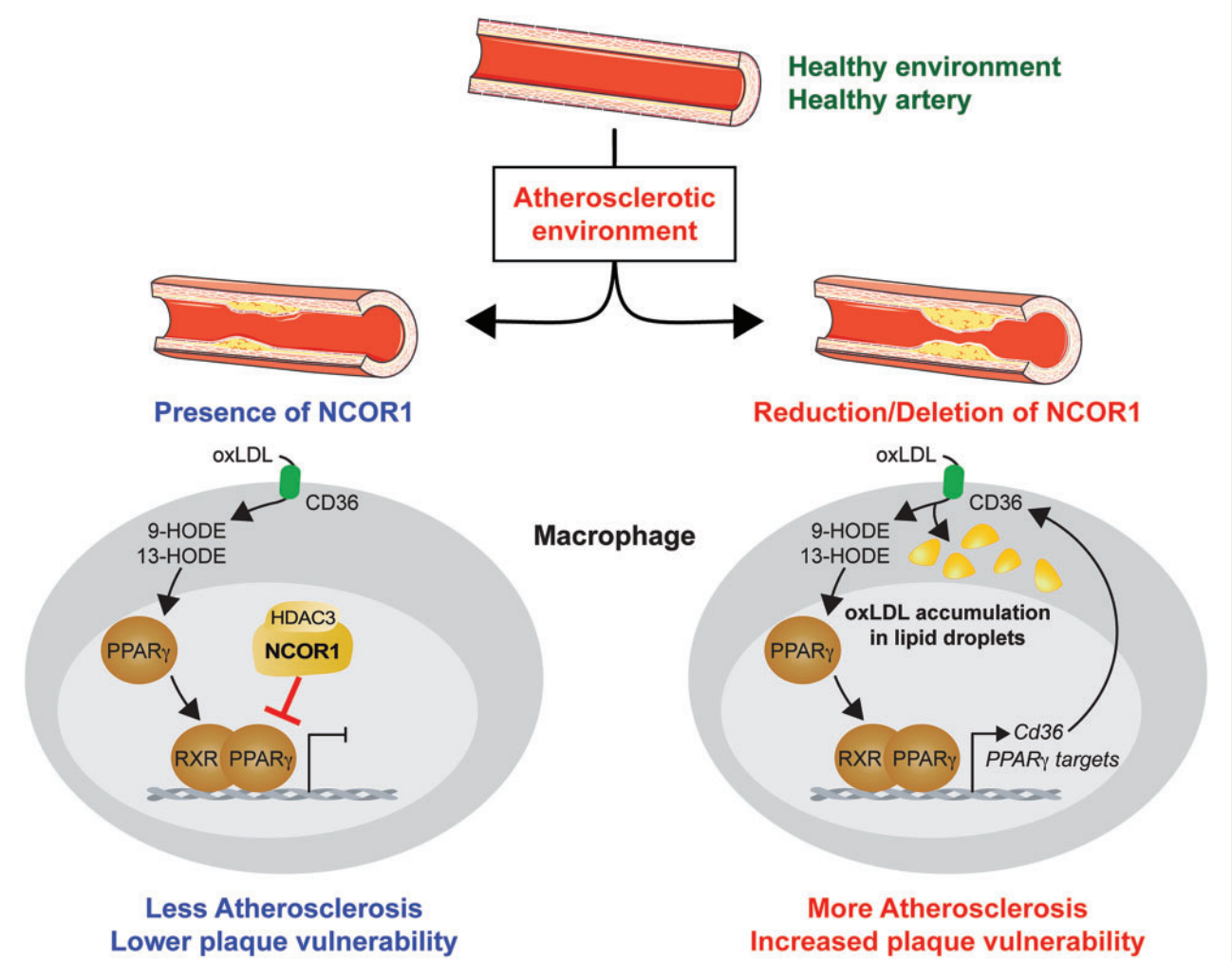

Take home figure Genetic deletion or silencing of macrophage Ncor1 leads to increased foam cell formation, enhanced expression of inflammatory cytokines, and the development of atherosclerotic lesions. The immunometabolic effects of NCOR1 are mediated via suppression of PPARγ target genes in mouse and human macrophages, which lead to an enhanced expression of the CD36 scavenger receptor and subsequent increase in oxLDL uptake in the absence of NCOR1.

Ruptured plaques are characterized by low NCOR1 vs. high CD36 expression

In a smaller scale-study, laser micro-dissected macrophages from ruptured and non-ruptured carotid plaques were analysed.[33] Interestingly, the expression of all significantly changed PPARγ target genes was robustly increased in macrophages from ruptured plaques (*Figure 6D*), and according to Lee *et al.*[33] PPARγ signalling was the most up-regulated pathway in ruptured compared with non-ruptured carotid plaques. We next made a rank of the top 500 *NCOR1*-coexpressed transcripts for two *NCOR1* probes from this dataset. These top *NCOR1*-coexpressed transcripts were then analysed for transcription factor-binding sites, and 69% of all correlates contain binding sites for PPARγ (*Figure 6E* and Supplementary material online, *Figure S16*). These data support the notion that NCOR1 also affects plaque development and stability in humans, which is in line with the increased signs of plaque vulnerability observed in the *L-Ncor1*$^{Mye-/-}$ mice (*Figure 1G–I*).

Since these human data were obtained from transcriptomic studies, we performed additional experiments to confirm our findings at the protein level. We first analysed PPARγ targets in internal controls, fatty streak regions and necrotic cores of plaques using unbiased tandem-mass spectrometry.[34] Five out of six detected PPARγ targets displayed a trend or significant increase in plaques compared with control regions (*Figure 6F*). Moreover, transcriptomic analyses revealed that PPARγ signalling is enriched in atherosclerotic arteries from the STAGE and laser micro-dissected macrophage datasets (Supplementary material online, *Table S2–S4*). Finally, in a targeted western blot, we detected less NCOR1 and more CD36 in ruptured compare to non-ruptured carotid plaques (*Figure 6G–I* and Supplementary material online, *Figure S17*). Consistently, a reverse causal reasoning computational approach study predicted that the

function of NCOR1 is reduced in both human and mouse advanced atherosclerotic plaques.[35] Taken together our data demonstrate that macrophage NCOR1 exerts its protective effects in atherosclerosis primarily via suppression of the vicious oxLDL–PPARγ–CD36 cycle (*Figure 6J* and *take home figure*).

Discussion

Our data demonstrate that NCOR1 mediates the repression of direct PPARγ target genes as well as the PPARγ-mediated repression of NF-κB and AP-1 and their pro-inflammatory target genes. In fact, our data suggest that NCOR1 is required for the nuclear receptor-mediated transrepression of inflammatory molecules.[16,17] The repression of direct PPARγ genes in macrophages, especially of CD36, is even more pronounced. A similar observation was made in adipocytes, where the deletion of *Ncor1* led to an enhanced activity of PPARγ and thus to an improved insulin sensitivity in high-fat diet fed mice.[9] Interestingly, the same group showed that also adipose-tissue macrophages improve insulin sensitivity in high-fat diet fed mice due to an enhanced synthesis of omega 3 fatty acids.[5]

Our study displays some scientific limitations. First, our causality work comes mainly from experiments in animal models and cell lines, while studying human specimens in most cases provide only associative evidence. Second, not all PPARγ target genes were altered in NCOR1-deficient macrophages due to the fact that many of these targets are highly expressed and regulated in a tissue-specific manner. For example, FABP4 is highly expressed and regulated in adipose tissue; in contrast, it is only modestly expressed in macrophages, but its mRNA expression can be induced upon PPARγ activation.[36] Future studies have to be carried out to analyse whether the beneficial effects of NCOR1 are mainly mediated via inhibition of direct PPARγ target genes, such as CD36, or via the PPARγ-mediated repression of pro-inflammatory transcription factors, such as NF-kB. Although we performed a series of experiments to show the causal role of CD36 to the increased accumulation of oxLDL *ex vivo*, the causal role of CD36 to the observed phenotype *in vivo* remains to be verified. The same holds true for other PPARγ-driven mechanisms, such as the alternative macrophages polarization, which does not seem to play a major (protective) role in our disease model, but could be very relevant in other conditions, such as in diet-induced obesity.[5]

Although PPARγ exerts beneficial insulin sensitizing functions in the adipose tissue, the role of macrophage PPARγ in cardiovascular disease has been discussed controversially.[37] Although experimental studies demonstrated that the activation of macrophage PPARγ exerts protective functions in atherosclerosis, others reported that PPARγ has pro-inflammatory functions and promotes atherogenesis.[37] Noteworthy, the pharmacological agonists have PPARγ-independent effects or beneficial PPARγ-dependent functions in other organs, such as insulin sensitization in adipose tissue.[38,39] Importantly, clinical trials using the PPARγ agonist rosiglitazone to treat type 2 diabetic patients were not successful due to an increased incidence of myocardial infarction, heart failure, and cardiovascular mortality.[40] Another trial using the PPARγ agonist pioglitazone was positive,[41] possibly due to additional off target effects mediated via PPARα activation.[42,43] Therefore, our data provide a possible explanation of the inconsistent and mainly disappointing results of clinical trials using PPARγ agonists by focusing selectively on macrophages, a primary player in plaque formation. Finally, our data suggest that stabilizing the NCOR1–PPARγ binding could be a promising strategy to uncouple beneficial from detrimental PPARγ-mediated effects and thereby block the pro-atherogenic functions of plaque macrophages, e.g. by suppressing the vicious oxLDL–PPARγ–CD36 cycle.

The defined function of macrophage NCOR1 in atherosclerosis may open new therapeutic strategies to prevent the development and progression of the atherosclerosis and cardiovascular disease. Indeed, it could offer an attractive way of fine-tuning the function of PPARγ in macrophages and thus preventing macrophage foam cell formation within arterial lesions, the development of atherosclerosis, and the rupture of vulnerable plaques.

Supplementary material

Supplementary material is available at *European Heart Journal* online.

Acknowledgements

We thank Johan Auwerx and Kristina Schoonjans from the École Polytechnique Fédérale de Lausanne for providing the floxed *Ncor1* mice, Trijnie Bos from the University of Groningen for excellent technical support with lipid analyses, and Wino Wijnen from WiWright for image acquisition of the stained *en face* aortae.

Funding

This study was supported by grants from the Swiss National Science Foundation (grant number PZOOP3_161521 to S.S., PZOOP3_161506 and PR00P3_179861/1 to E.O.); the Novartis Foundation for medical-biological Research (grant number 16B103 to S.S.); the Swiss Life Foundation to S.S.; the Olga-Mayenfisch Foundation to S.S.; the OPO foundation (grant number 2018-0054 to S.S.); the Swiss Heart Foundation to S.N.-S.; and the Zurich Heart House—Foundation for Cardiovascular Research, Zurich to S.N.-S. M.H.O holds a Rosalind Franklin Fellowship from the University of Groningen.

Conflict of interest: none declared.

References

1. Weber C, Noels H. Atherosclerosis: current pathogenesis and therapeutic options. *Nature Medicine* 2011;**17**:1410–1422.
2. Swirski FK, Nahrendorf M. Leukocyte behavior in atherosclerosis, myocardial infarction, and heart failure. *Science* 2013;**339**:161–166.
3. Mottis A, Mouchiroud L, Auwerx J. Emerging roles of the corepressors NCoR1 and SMRT in homeostasis. *Genes Dev* 2013;**27**:819–835.
4. Jepsen K, Hermanson O, Onami TM, Gleiberman AS, Lunyak V, McEvilly RJ, Kurokawa R, Kumar V, Liu F, Seto E, Hedrick SM, Mandel G, Glass CK, Rose DW, Rosenfeld MG. Combinatorial roles of the nuclear receptor corepressor in transcription and development. *Cell* 2000;**102**:753–763.
5. Li P, Spann NJ, Kaikkonen MU, Lu M, Oh da Y, Fox JN, Bandyopadhyay G, Talukdar S, Xu J, Lagakos WS, Patsouris D, Armando A, Quehenberger O, Dennis EA, Watkins SM, Auwerx J, Glass CK, Olefsky JM. NCoR repression of LXRs restricts macrophage biosynthesis of insulin-sensitizing omega 3 fatty acids. *Cell* 2013;**155**:200–214.
6. Jo YS, Ryu D, Maida A, Wang X, Evans RM, Schoonjans K, Auwerx J. Phosphorylation of the nuclear receptor corepressor 1 by protein kinase B switches its corepressor targets in the liver in mice. *Hepatology* 2015;**62**:1606–1618.
7. Astapova I, Ramadoss P, Costa-e-Sousa RH, Ye F, Holtz KA, Li Y, Niepel MW, Cohen DE, Hollenberg AN. Hepatic nuclear corepressor 1 regulates cholesterol absorption through a TRβ1-governed pathway. *J Clin Invest* 2014;**124**:1976–1986.
8. Yamamoto H, Williams EG, Mouchiroud L, Canto C, Fan W, Downes M, Heligon C, Barish GD, Desvergne B, Evans RM, Schoonjans K, Auwerx J. NCoR1

is a conserved physiological modulator of muscle mass and oxidative function. *Cell* 2011;**147**:827–839.
9. Li P, Fan W, Xu J, Lu M, Yamamoto H, Auwerx J, Sears DD, Talukdar S, Oh D, Chen A, Bandyopadhyay G, Scadeng M, Ofrecio JM, Nalbandian S, Olefsky JM. Adipocyte NCoR knockout decreases PPARγ phosphorylation and enhances PPARγ activity and insulin sensitivity. *Cell* 2011;**147**:815–826.
10. Clausen BE, Burkhardt C, Reith W, Renkawitz R, Forster I. Conditional gene targeting in macrophages and granulocytes using LysMcre mice. *Transgenic Res* 1999;**8**:265–277.
11. Ishibashi S, Brown MS, Goldstein JL, Gerard RD, Hammer RE, Herz J. Hypercholesterolemia in low density lipoprotein receptor knockout mice and its reversal by adenovirus-mediated gene delivery. *J Clin Invest* 1993;**92**:883–893.
12. Müller A, Mu L, Meletta R, Beck K, Rancic Z, Drandarov K, Kaufmann PA, Ametamey SM, Schibli R, Borel N, Kramer SD. Towards non-invasive imaging of vulnerable atherosclerotic plaques by targeting co-stimulatory molecules. *Int J Cardiol* 2014;**174**:503–515.
13. Pedretti M, Rancic Z, Soltermann A, Herzog BA, Schliemann C, Lachat M, Neri D, Kaufmann PA. Comparative immunohistochemical staining of atherosclerotic plaques using F16, F8 and L19: three clinical-grade fully human antibodies. *Atherosclerosis* 2010;**208**:382–389.
14. Stary HC, Chandler AB, Dinsmore RE, Fuster V, Glagov S, Insull W Jr, Rosenfeld ME, Schwartz CJ, Wagner WD, Wissler RW. A definition of advanced types of atherosclerotic lesions and a histological classification of atherosclerosis. A report from the Committee on Vascular Lesions of the Council on Arteriosclerosis, American Heart Association. *Arterioscler Thromb Vasc Biol* 1995;**15**:1512–1531.
15. Ghisletti S, Huang W, Ogawa S, Pascual G, Lin ME, Willson TM, Rosenfeld MG, Glass CK. Parallel SUMOylation-dependent pathways mediate gene- and signal-specific transrepression by LXRs and PPARgamma. *Mol Cell* 2007;**25**:57–70.
16. Ghisletti S, Huang W, Jepsen K, Benner C, Hardiman G, Rosenfeld MG, Glass CK. Cooperative NCoR/SMRT interactions establish a corepressor-based strategy for integration of inflammatory and anti-inflammatory signaling pathways. *Genes Dev* 2009;**23**:681–693.
17. Pascual G, Fong AL, Ogawa S, Gamliel A, Li AC, Perissi V, Rose DW, Willson TM, Rosenfeld MG, Glass CK. A SUMOylation-dependent pathway mediates transrepression of inflammatory response genes by PPAR-gamma. *Nature* 2005;**437**:759–763.
18. Folkersen L, Persson J, Ekstrand J, Agardh HE, Hansson GK, Gabrielsen A, Hedin U, Paulsson-Berne G. Prediction of ischemic events on the basis of transcriptomic and genomic profiling in patients undergoing carotid endarterectomy. *Mol Med* 2012;**18**:669–675.
19. Doring Y, Drechsler M, Soehnlein O, Weber C. Neutrophils in atherosclerosis: from mice to man. *Arterioscler Thromb Vasc Biol* 2015;**35**:288–295.
20. Silverstein RL, Febbraio M. CD36, a scavenger receptor involved in immunity, metabolism, angiogenesis, and behavior. *Sci Signal* 2009;**2**:re3.
21. Febbraio M, Podrez EA, Smith JD, Hajjar DP, Hazen SL, Hoff HF, Sharma K, Silverstein RL. Targeted disruption of the class B scavenger receptor CD36 protects against atherosclerotic lesion development in mice. *J Clin Invest* 2000;**105**:1049–1056.
22. Endemann G, Stanton LW, Madden KS, Bryant CM, White RT, Protter AA. CD36 is a receptor for oxidized low density lipoprotein. *J Biol Chem* 1993;**268**:11811–11816.
23. Barish GD, Yu RT, Karunasiri MS, Becerra D, Kim J, Tseng TW, Tai LJ, Leblanc M, Diehl C, Cerchietti L, Miller YI, Witztum JL, Melnick AM, Dent AL, Tangirala RK, Evans RM. The Bcl6-SMRT/NCoR cistrome represses inflammation to attenuate atherosclerosis. *Cell Metab* 2012;**15**:554–562.
24. Lefterova MI, Steger DJ, Zhuo D, Qatanani M, Mullican SE, Tuteja G, Manduchi E, Grant GR, Lazar MA. Cell-specific determinants of peroxisome proliferator-activated receptor gamma function in adipocytes and macrophages. *Mol Cell Biol* 2010;**30**:2078–2089.
25. Coort SL, Willems J, Coumans WA, van der Vusse GJ, Bonen A, Glatz JF, Luiken JJ. Sulfo-N-succinimidyl esters of long chain fatty acids specifically inhibit fatty acid translocase (FAT/CD36)-mediated cellular fatty acid uptake. *Mol Cell Biochem* 2002;**239**:213–219.
26. Li AC, Brown KK, Silvestre MJ, Willson TM, Palinski W, Glass CK. Peroxisome proliferator-activated receptor gamma ligands inhibit development of atherosclerosis in LDL receptor-deficient mice. *J Clin Invest* 2000;**106**:523–531.
27. Nagy L, Tontonoz P, Alvarez JG, Chen H, Evans RM. Oxidized LDL regulates macrophage gene expression through ligand activation of PPARgamma. *Cell* 1998;**93**:229–240.
28. Tontonoz P, Nagy L, Alvarez JG, Thomazy VA, Evans RM. PPARgamma promotes monocyte/macrophage differentiation and uptake of oxidized LDL. *Cell* 1998;**93**:241–252.
29. Rigamonti E, Chinetti-Gbaguidi G, Staels B. Regulation of macrophage functions by PPAR-alpha, PPAR-gamma, and LXRs in mice and men. *Arterioscler Thromb Vasc Biol* 2008;**28**:1050–1059.
30. King KL, Stanley WC, Rosca M, Kerner J, Hoppel CL, Febbraio M. Fatty acid oxidation in cardiac and skeletal muscle mitochondria is unaffected by deletion of CD36. *Arch Biochem Biophys* 2007;**467**:234–238.
31. Yang S, Kim CY, Hwang S, Kim E, Kim H, Shim H, Lee I. COEXPEDIA: exploring biomedical hypotheses via co-expressions associated with medical subject headings (MeSH). *Nucleic Acids Res* 2017;**45**:D389–D396.
32. Hagg S, Skogsberg J, Lundstrom J, Noori P, Nilsson R, Zhong H, Maleki S, Shang MM, Brinne B, Bradshaw M, Bajic VB, Samnegard A, Silveira A, Kaplan LM, Gigante B, Leander K, de Faire U, Rosfors S, Lockowandt U, Liska J, Konrad P, Takolander R, Franco-Cereceda A, Schadt EE, Ivert T, Hamsten A, Tegner J, Bjorkegren J. Multi-organ expression profiling uncovers a gene module in coronary artery disease involving transendothelial migration of leukocytes and LIM domain binding 2: the Stockholm Atherosclerosis Gene Expression (STAGE) study. *PLoS Genet* 2009;**5**:e1000754.
33. Lee K, Santibanez-Koref M, Polvikoski T, Birchall D, Mendelow AD, Keavney B. Increased expression of fatty acid binding protein 4 and leptin in resident macrophages characterises atherosclerotic plaque rupture. *Atherosclerosis* 2013;**226**:74–81.
34. Liang W, Ward LJ, Karlsson H, Ljunggren SA, Li W, Lindahl M, Yuan XM. Distinctive proteomic profiles among different regions of human carotid plaques in men and women. *Sci Rep* 2016;**6**:26231.
35. De Leon H, Boue S, Schlage WK, Boukharov N, Westra JW, Gebel S, VanHooser A, Talikka M, Fields RB, Veljkovic E, Peck MJ, Mathis C, Hoang V, Poussin C, Deehan R, Stolle K, Hoeng J, Peitsch MC. A vascular biology network model focused on inflammatory processes to investigate atherogenesis and plaque instability. *J Transl Med* 2014;**12**:185.
36. Hotamisligil GS, Bernlohr DA. Metabolic functions of FABPs-mechanisms and therapeutic implications. *Nat Rev Endocrinol* 2015;**11**:592–605.
37. Chawla A. Control of macrophage activation and function by PPARs. *Circ Res* 2010;**106**:1559–1569.
38. Cariou B, Charbonnel B, Staels B. Thiazolidinediones and PPARγ agonists: time for a reassessment. *Trends Endocrinol Metab* 2012;**23**:205–215.
39. Chawla A, Barak Y, Nagy L, Liao D, Tontonoz P, Evans RM. PPAR-γ dependent and independent effects on macrophage-gene expression in lipid metabolism and inflammation. *Nat Medicine* 2001;**7**:48–52.
40. Nissen SE, Wolski K. Effect of rosiglitazone on the risk of myocardial infarction and death from cardiovascular causes. *N Engl J Med* 2007;**356**:2457–2471.
41. Kernan WN, Viscoli CM, Furie KL, Young LH, Inzucchi SE, Gorman M, Guarino PD, Lovejoy AM, Peduzzi PN, Conwit R, Brass LM, Schwartz GG, Adams HP Jr, Berger L, Carolei A, Clark W, Coull B, Ford GA, Kleindorfer D, O'Leary JR, Parsons MW, Ringleb P, Sen S, Spence JD, Tanne D, Wang D, Winder TR; IRIS Trial Investigators. Pioglitazone after ischemic stroke or transient ischemic attack. *N Engl J Med* 2016;**374**:1321–1331.
42. Sakamoto J, Kimura H, Moriyama S, Odaka H, Momose Y, Sugiyama Y, Sawada H. Activation of human peroxisome proliferator-activated receptor (PPAR) subtypes by pioglitazone. *Biochem Biophys Res Commun* 2000;**278**:704–711.
43. Hirakata M, Tozawa R, Imura Y, Sugiyama Y. Comparison of the effects of pioglitazone and rosiglitazone on macrophage foam cell formation. *Biochem Biophys Res Commun* 2004;**323**:782–788.